PROCEEDINGS B

royalsocietypublishing.org/journal/rspb

Research

Cite this article: Rauscher MJ, Fox JL. 2021 Haltere and visual inputs sum linearly to predict wing (but not gaze) motor output in tethered flying *Drosophila*. *Proc. R. Soc. B* **288**: 20202374.
https://doi.org/10.1098/rspb.2020.2374

Received: 23 September 2020
Accepted: 16 December 2020

Subject Category:
Behaviour

Subject Areas:
behaviour, neuroscience

Keywords:
Drosophila, haltere, multisensory integration, insect flight, gaze control

Author for correspondence:
Jessica L. Fox
e-mail: jlf88@case.edu

Electronic supplementary material is available online at https://doi.org/10.6084/m9.figshare.c.5271387.

THE ROYAL SOCIETY PUBLISHING

Haltere and visual inputs sum linearly to predict wing (but not gaze) motor output in tethered flying *Drosophila*

Michael J. Rauscher and Jessica L. Fox

Department of Biology, Case Western Reserve University, Cleveland, OH 44106-7080, USA

MJR, 0000-0002-0607-1083; JLF, 0000-0001-6374-657X

In the true flies (Diptera), the hind wings have evolved into specialized mechanosensory organs known as halteres, which are sensitive to gyroscopic and other inertial forces. Together with the fly's visual system, the halteres direct head and wing movements through a suite of equilibrium reflexes that are crucial to the fly's ability to maintain stable flight. As in other animals (including humans), this presents challenges to the nervous system as equilibrium reflexes driven by the inertial sensory system must be integrated with those driven by the visual system in order to control an overlapping pool of motor outputs shared between the two of them. Here, we introduce an experimental paradigm for reproducibly altering haltere stroke kinematics and use it to quantify multisensory integration of wing and gaze equilibrium reflexes. We show that multisensory wing-steering responses reflect a linear superposition of haltere-driven and visually driven responses, but that multisensory gaze responses are not well predicted by this framework. These models, based on populations, extend also to the responses of individual flies.

1. Introduction

Many animals have stabilizing equilibrium reflexes that are active during both self-generated and externally imposed movements [1]. Complementary versions of these reflexes are driven by visual and inertial sensory systems, and a major task of the nervous system is to appropriately coordinate these interconnected sensorimotor streams. In the true flies (Diptera), wing-steering and gaze control equilibrium reflexes essential to stable flight are mediated by the compound eyes (as in other insects) and by unique vestibular-like organs known as halteres. Long known to be necessary for stable flight [2,3], halteres are a pair of reduced hindwings that beat in time with the lift-generating forewings and actively sense inertial forces via fields of campaniform sensilla [4–6]. The neurons underlying these sensilla fire with close fidelity to the haltere's stroke cycle and are capable of representing the stroke amplitude and plane of oscillation with sub-millisecond precision [3,7,8]. Fast monosynaptic thoracic microcircuits linking haltere campaniforms to ipsilateral head- and wing-steering motoneurons have been characterized in reduced preparation [9–12], and interneurons linking contralateral haltere campaniforms to these targets have been described anatomically (but not functionally; [13]).

These head- and wing-steering motoneurons also receive inputs from descending neurons conveying visual motion information [10,11,13] that has been decomposed into component vectors that align with the control axis of each downstream motoneuron and its associated muscle [14]. This 'matched filter' model has been explored extensively for the motoneurons controlling head movements [10], and a similar scheme is thought to be employed in the control of wingstroke amplitude [15–17]. By contrast, haltere campaniform neurons project either monosynaptically or via a single interneuron to these same synaptic targets [9,18,19]. There are no further loci for signals from the two sensory modalities to be brought into registration with one another

before producing a motor output. This suggests that a similar decomposition of motion information from the halteres into component vectors matched with each motoneuron's axis of control is accomplished with minimal processing via a population vector coding scheme [7,8]. Calcium imaging of the ascending projections of the haltere nerve into the neck connectives supports this, showing distinct and overlapping patterns of fluorescence emerging in conjunction with steering manoeuvres [20].

Consequently, the two sensory systems likely encode self-motion cues within the same coordinate frame. Using a tethered flight arena mounted in a multi-axial gimbal, Sherman and Dickinson identified an overlapping range of rotational velocity cues that provoke wing-steering responses of similar amplitude from each sensory system, with the two systems capable of detecting differences in the phase of periodically varying stimuli presented to them concurrently [21–23]. These and other tethered flight experiments also showed that animals with surgically ablated halteres lose the ability to modulate their wingbeat amplitude and frequency in response to imposed motion [21,24]. Similarly, studies of gaze stabilization in blowflies show that while halteres mediate responses to faster rotational stimuli than the visual system, the two sensory systems elicit head rolls with similar amplitudes over the overlapping range of stimulus velocities where they are both responsive [25]. Subsequent experiments in *Drosophila* show that haltere ablation renders these animals incapable of modulating the amplitude of their gaze responses to different visual pattern velocities [26].

While ablation experiments demonstrate the effects of complete sensory loss, they are limited in their ability to reveal the functional details of the haltere sensory system. In the intact, behaving animal, kinematic outputs are the result of cues from both halteres and vision and the tight network of feedback they share with one another. One strategy for characterizing such densely interconnected systems is to introduce small (but not destabilizing) changes to key parameters of one of multiple inputs in order to quantify changes in the system's output, as exemplified by Bender and Dickinson's experiments manipulating the weight of the haltere bulb (the 'proof mass' of the system) and observing changes to the dynamics of fast visually evoked saccades [27]. While the haltere's unique anatomy makes such experiments conceptually viable, its extreme sensitivity to small inertial forces—which has made halteres an excellent system for studying the encoding properties of individual campaniform sensilla—paradoxically makes such experiments difficult to achieve practically. Biomechanical modelling suggests that the naturalistic range of forces acting on the haltere during the flight is very small, of the order of 10^{-8} N [28], with stroke plane and amplitude deviations in the haltere's path resulting from body rotations on the order of microns [29]. Manipulation of the system at this scale is clearly desirable towards the goal of understanding functional aspects of haltere biomechanics.

Here, we alter haltere kinematics in a reproducible and measurable fashion. By gluing small iron filings to the haltere and tethering the fly in an electromagnetic field, we gently modulated the haltere's stroke and observed the effects of this manipulation on the fly's head and wing movement behaviour. In doing so, we quantify the behaviours elicited by specific movements of the haltere. We show that haltere-elicited and visually elicited wing amplitude responses sum linearly as a superposition of states. Contrastingly, we show that head movement responses to the two sensory modalities predominately reflect the influence of vision. We demonstrate that our analysis performs well for individual animals as well as the larger dataset.

2. Results

(a) Haltere loading alters stroke amplitude and frequency

Prior to using the electromagnet to move the haltere, we needed to establish a baseline iron filing mass that would not disrupt the haltere's natural stroke. Similar to the halteres of most other flies, *Drosophila* halteres maintain a characteristic antiphase synchrony with the wingstroke and a stroke amplitude of 140–220° [30,31]. To evaluate the influence of haltere loading on haltere stroke kinematics, we applied UV-curing dental cement and iron filings of various sizes to the halteres of 155 flies and tracked haltere movements using high-speed videography (figure 1*a*). We found that smaller masses (below approximately 12 µg) permitted a naturalistic stroke amplitude and frequency, whereas larger masses reduced the stroke amplitude of the beating haltere and lowered its stroke frequency, breaking the haltere's characteristic synchrony with the wing (figure 1*b*). These results complement prior experiments on the black soldier fly, which found that halteres are weakly mechanically linked with one another and more strongly linked with the wings [31] and that additional bulb mass can cause one of the halteres to adopt a different stroke frequency from the wing [32].

(b) Increasing the haltere loading using the electromagnet induces compensatory wing- and head-steering reflexes

After identifying a threshold of additional bulb mass that would not limit the haltere's stroke amplitude or compromise its synchrony with the wing, we conducted experiments using flies treated with filings within this range. This facilitated control over the haltere movement via an electromagnet (figure 1*a*) located posteriorly and ventrally to the fly with a field strength at the haltere of approximately 2000 µT when fully energized (electronic supplementary material, figure S1). In 120 repeated trials across 13 flies (3–12 trials per fly), we activated the electromagnet for 250 ms and observed an average reduction of the haltere stroke amplitude of approximately 15°. Flies without an iron filing did not respond to the magnetic stimulation (electronic supplementary material, figure S2). For a subset of 80 trials, we also measured kinematics of the untreated opponent halteres and found their stroke amplitudes to be unaffected by application of the magnetic field (figure 1*c–f*, electronic supplementary material, video S1). Following each stimulation pulse, the stroke amplitude of the treated haltere returned to levels comparable to the pre-trial baseline.

Due to the high sensitivity of haltere afferent neurons to virtually any externally imposed movement [30], it is impossible to accurately ascribe a fictive rotational axis (yaw, pitch, or roll) that this manipulation might represent to the fly. Nevertheless, our manipulation does not appear to compromise the structure of the wing motor pattern; the characteristic

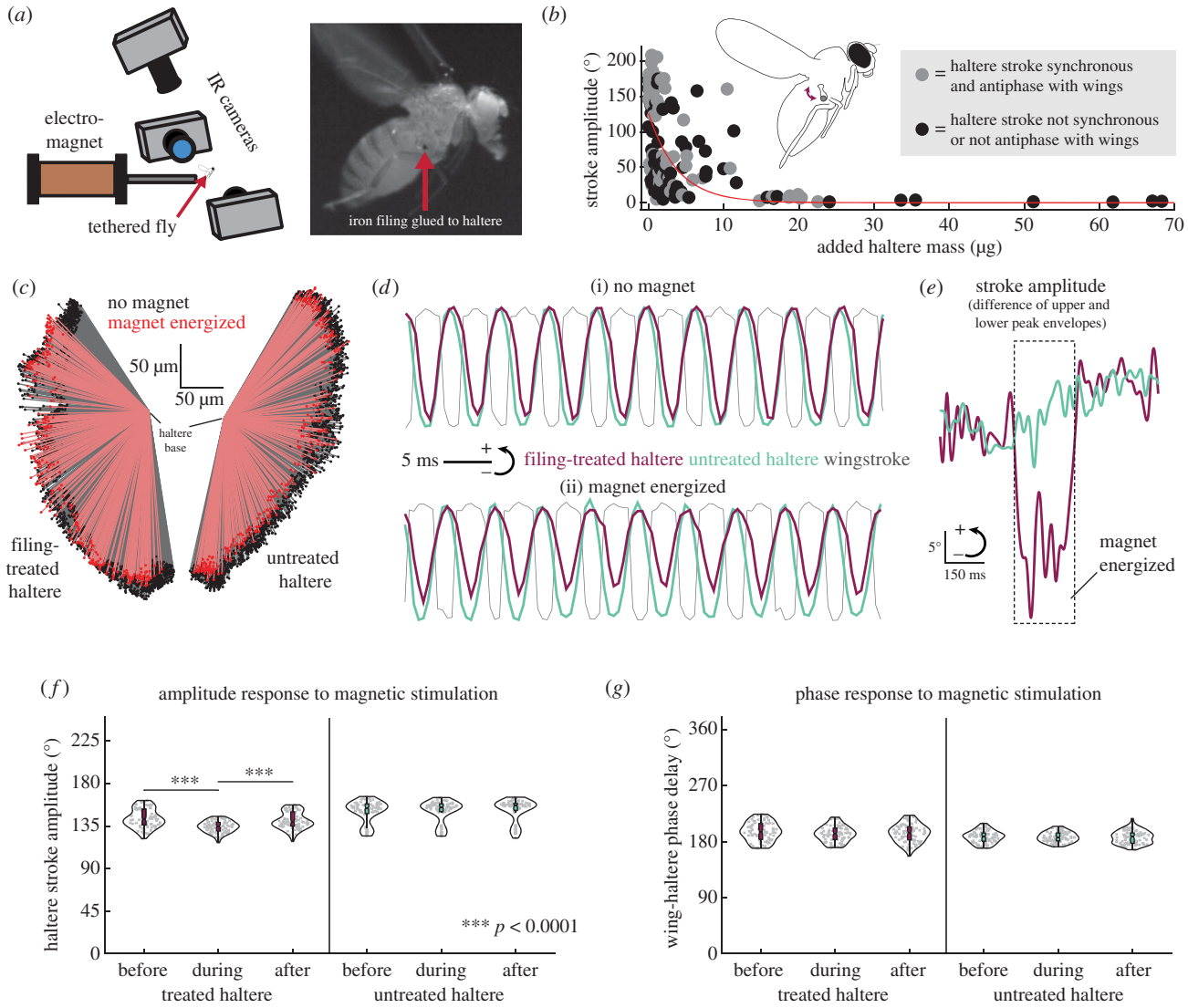

Figure 1. Electromagnetic control of haltere stroke kinematics. (*a*) Illustration of experimental set-up. Tethered flies were suspended between two electromagnets, enabling control over one of the two halteres via an iron filing attached to the bulb (*a*, inset). Haltere, wing and head kinematics were recorded using several high-speed IR cameras. (*b*) Amplitude response of haltere stroke to addition of bulb mass via UV-curing dental cement or iron filings (red: single-term exponential curve of best fit). Grey dots show animals for which the haltere stroke retained a naturalistic antiphase synchrony with the wings. Black dots show animals for which the haltere stroke either lost antiphase synchrony with the wings or adopted a different stroke frequency. Many animals accommodated a small amount of additional mass while retaining a full naturalistic stroke amplitude and frequency, and such animals were used for experiments changing the haltere stroke amplitude. Beyond 12 µg additional mass no haltere exhibited an appreciable stroke amplitude or frequency. (*c*) Haltere tracking from representative pulse epoch. Darker points (black) are pooled from tracking over a 250 ms window before the magnetic stimulation pulse and a matched window 250 ms after the conclusion of the pulse. Lighter points (red) are drawn from the stimulation pulse epoch, following the initial 50 ms period where the magnet is energizing. (*d*) Representative kinematic traces showing treated haltere, untreated haltere and wing stroke cycles for the same fly under baseline conditions (i) and with magnet energized (ii), showing preservation of haltere-wing phase relationship. Traces normalized to extrema of entire time series. (*e*) Representative traces showing change in treated haltere stroke amplitude (difference of upper and lower peak envelopes) for one animal with activation of magnetic stimulation. (*f*) Amplitude responses to magnetic stimulation for treated and untreated halteres, showing reduced stroke amplitude during the magnetic pulse epoch for the treated haltere only ($n = 80$ trials, *** $p < 0.0001$, Wilcoxon rank-sum test with Bonferroni correction for multiple comparisons). (*g*) Phase relationship with the wing is maintained during magnetic stimulation. See also the electronic supplementary material, video S1. (Online version in colour.)

antiphase synchrony between the wing and haltere strokes was maintained throughout each stimulus epoch and immediately following (figure 1*g*). At the same time, the magnetic stimulation of the haltere was also accompanied by a small (3 Hz) but consistent increase in the haltere stroke frequency (electronic supplementary material, figure S3A). In keeping with the observation that the wing-haltere stroke phase is maintained throughout the magnetic stimulation, this increase in stroke frequency is also observed in the untreated opponent haltere (electronic supplementary material, figure S3B) and the wing (electronic supplementary material, figure S3C). These findings are congruent with tethered flight experiments showing that halteres are necessary for wingbeat frequency modulation during steering manoeuvres [21,22], and corroborate wing muscle recordings in which optogenetic activation of the haltere motor system produces acute phase changes in the wing motor system [20].

To analyse the imposed haltere movement in more spatio-temporal detail, as well as quantify its influence on the head and wings, we produced event-triggered average (ETA) responses for the haltere stroke amplitude, wingstroke amplitudes and head yaw (schematized in figure 2*a*). Response

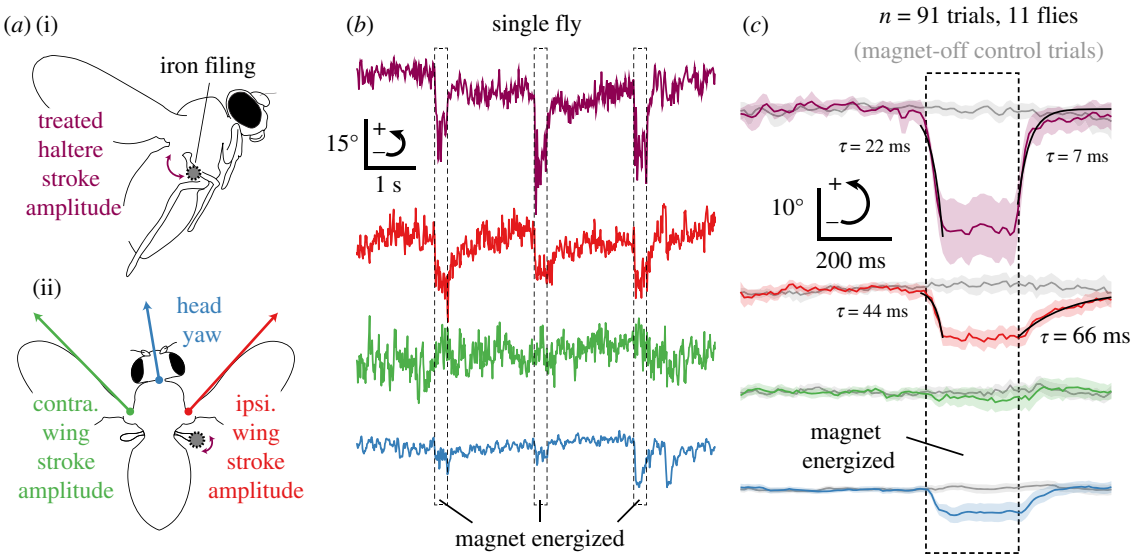

Figure 2. Reduction in haltere stroke amplitude induces compensatory head and wing responses. (*a*) Legend of measured kinematic parameters. Haltere stroke amplitude measured from lateral aspect camera (i), wingstroke amplitudes and head yaw measured from overhead camera (ii). (*b*) Several representative repeated trials from one animal subject, showing decrease in haltere stroke amplitude (top, difference of upper and lower peak envelopes) during magnetic stimulation and (in descending order) concurrent ipsilateral wing, contralateral wing, and head steering responses. (*c*) Event-triggered average of each measured kinematic parameter with 95% confidence intervals for all 91 trials, each zeroed on pre-magnet baseline. Means and confidence intervals in light grey depict time-matched control epochs with no magnetic stimulation drawn from the same videos as the experimental epochs. (Online version in colour.)

levels varied between individuals (electronic supplementary material, figure S4) but were qualitatively similar for 11 of the 13 flies (the remaining two are discussed below). In these animals, the induced reduction in haltere stroke amplitude caused a concurrent reduction of approximately 10° in the stroke amplitude of the ipsilateral wing as well as a head yaw of approximately 5° toward the direction of the treated haltere (figure 2*b*,*c*). To quantify the time course of response to the haltere stimulation, we fit exponential curves to the haltere and ipsilateral wing ETAs over the initial magnetic stimulus period (figure 2*c*). We found that onset of the magnetic stimulation produces a drop in haltere stroke amplitude with a comparatively short-time constant ($\tau =$ 22 ms), with the induced changes in wingstroke amplitude following with a slower time constant ($\tau = 44$ ms). We found a similar pattern with models fit the post-stimulus recovery for both parameters ($\tau = 7$ ms and 66 ms for the haltere and wing stroke amplitude, respectively). The magnets were not synchronized to turn on at a specific phase of the fly's wingbeat and the particular phase at which the magnet was activated did not affect the fly's response (electronic supplementary material, figure S5).

In the two remaining flies, we observed distinct responses that were consistent and repeatable for each individual. In one of them, the ipsilateral wingstroke amplitude increased, rather than decreased, during bouts of magnetic stimulation (fly 6, electronic supplementary material, figure S4). In the other fly, the head movement response was inverted, with the head yawing toward the direction of the untreated contralateral haltere (fly 8, electronic supplementary material, figure S4). This fly also exhibited an increase in contralateral wing downstroke amplitude during the magnetic stimulation periods. Despite these different responses, the same analysis conducted in the following sections illustrates a common mechanism at work across the dataset (see below, 'Linear models predict the responses of individual flies as well as the mean').

(c) Haltere-induced steering responses sum linearly with concurrent visual responses for head and wings

To investigate how haltere-evoked steering responses are integrated with visually evoked steering responses, we repeated the experiments above while also stimulating the fly's visual system with a wide-field grating pattern moving in the yaw plane (see Methods). Because we cannot definitively ascribe a fictive rotational axis that our haltere manipulation would represent to the fly beyond the inherent asymmetry of stimulating only one haltere, we chose this visual stimulus because it would require asymmetric coordination of motor output across the body axis and because it was known to reliably evoke robust compensatory optomotor steering responses in the head and wings. A fictive roll manoeuvre would also meet these criteria; indeed, tethered flies show similar responses to roll and yaw visual stimuli [33]. In our stimulation protocol, the visual stimulus moved about the yaw axis of the fly in a triangle-wave pattern, and the halteres were stimulated with the magnet while the pattern moved either clockwise (figure 3*a*,*c*,*e*,*g*) or anticlockwise (figure 3*b*,*d*,*f*,*h*). For each fly, repeated trials of concurrent visual and magnetic stimulation were interleaved with visual-only control trials, during which the magnet was off.

The magnetic stimulation did not compromise the ability of flies to steer their head and wings in response to either directional category of visual stimulus. As above, we observed a reduction in the ipsilateral wing downstroke amplitude during the magnetic stimulation bouts, outside of the confidence intervals of the visual-stimulus-only control (figure 3*c*,*d*). Unlike the haltere-only condition, we did not observe a head yaw in the direction of the treated haltere outside the confidence interval of the visual-stimulus-only baseline. To assess the multisensory integration of haltere and visual information, we created a summation model for each kinematic parameter. We summed the unweighted ETA

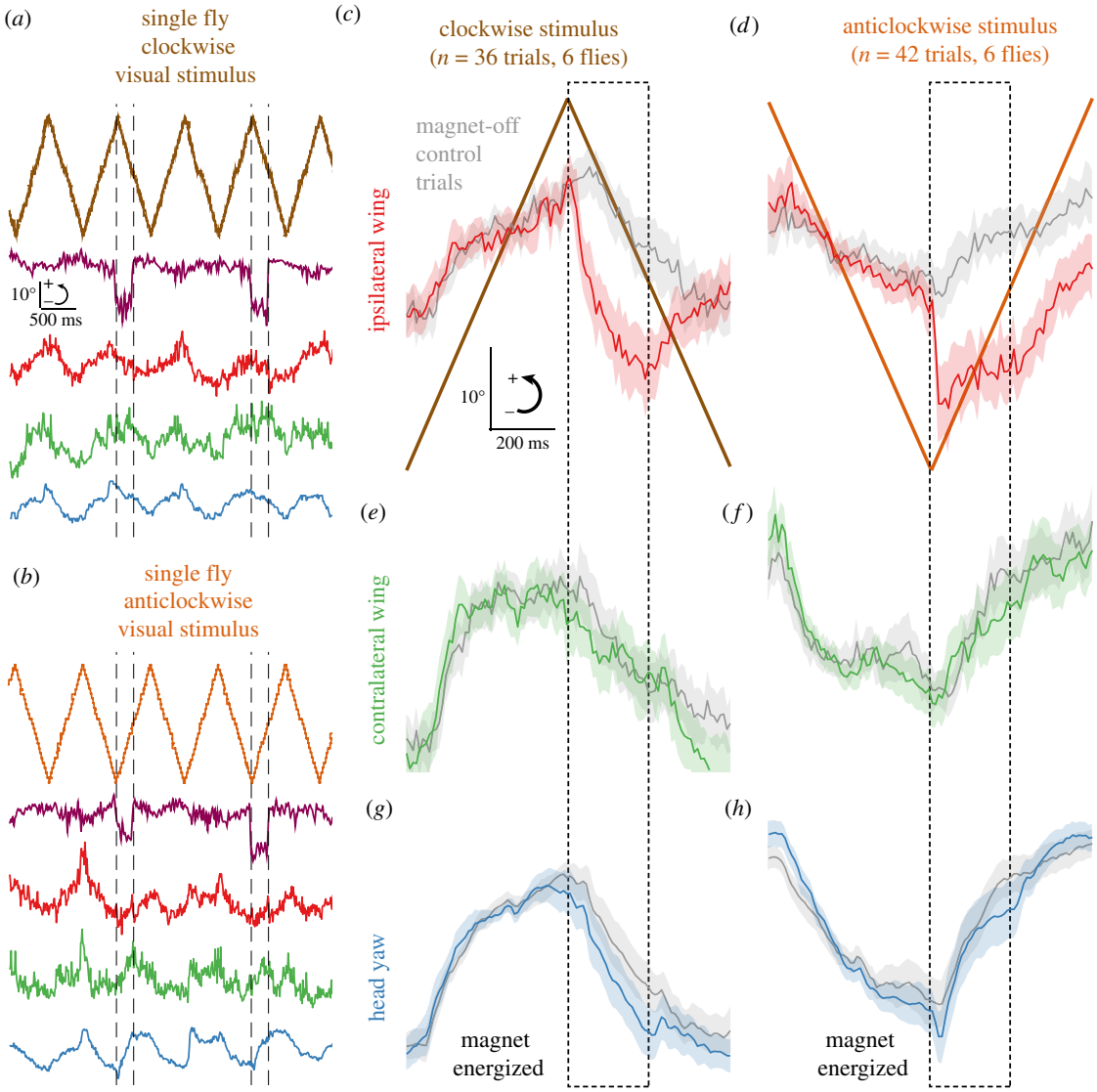

Figure 3. Response to concurrent haltere and visual sensory inputs. (*a*) Representative kinematic traces from one animal subject responding to clockwise visual and haltere stimuli, showing the same kinematic parameters in same presentation order as depicted in figure 2. Note robust optomotor steering response for all kinematic parameters. (*b*) Same as (*a*), but for anticlockwise visual stimulus. (*c–h*) Event-triggered average wing and head responses for all flies with visual stimulus epochs. (*c,e,g*) Clockwise trials ($n = 36$ trials, six flies). (*d,f,h*) Anticlockwise trials ($n = 42$ trials, six flies). (Online version in colour.)

of the visual-stimulation-only trials with the unweighted ETA from the haltere-stimulation-only trials from the same flies, fitting only an intercept to minimize error. For comparison, we also performed a conventional multiple linear regression (MLR) analysis that fit weighted coefficients to each predictor and also permitted us to quantify the relative contribution of each predictor variable to the explained variance of the model by computing componentized ANOVA statistics. We refer to these two classes of models as 'unweighted' and 'weighted' models for the remainder of the manuscript.

For all kinematic parameters, we found that both the unweighted and weighted models predicted the observed steering responses for concurrent stimulation of both sensory modalities with comparable R^2 values (figure 4*a–f*). This was unsurprising for the contralateral wing (figure 4*b,e*) and head (figure 4*c,f*) responses, which were dominated by the visual component, but was most striking for the ipsilateral wing-steering response (figure 4*a,d*). The comparable performances of the unweighted and weighted models suggest that the total ipsilateral wing-steering output reflects a linear superposition of haltere-evoked and visually evoked components. Models are summarized in electronic supplementary material, tables S1 and S2 for clockwise and anticlockwise trials respectively.

A straightforward prediction of the unweighted model is that the visually evoked components of the clockwise and anticlockwise responses should differ only in their signs. To test this, we constructed a model that averaged the clockwise and anticlockwise multisensory ETAs, expecting that the visual components should cancel and predict the response evoked by the haltere stimulus only (as shown in figure 2). As above, we also compared this unweighted model to a conventional weighted model. These models are summarized in electronic supplementary material, table S3.

In keeping with the linear superposition hypothesis, we found that both models strongly predict the haltere-evoked ipsilateral wing-steering response (figure 4*c*). As expected, both models performed poorly in predicting the contralateral wing response (figure 4*h*): because the contralateral wing did not respond to the haltere stimulation, any correlation would be a result of random error. The modest increases in the weighted model performance over the unweighted model are therefore likely the result of overfitting.

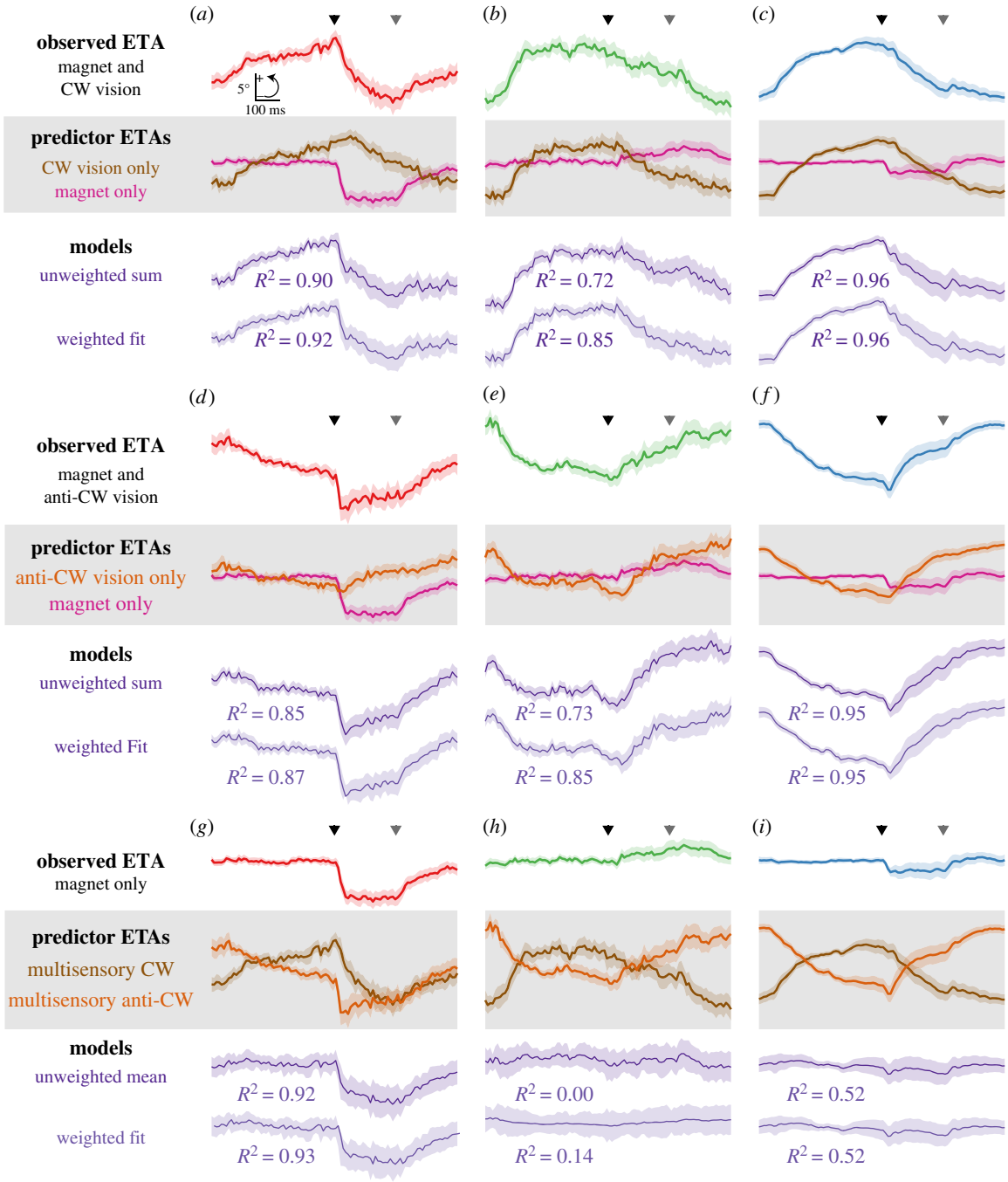

Figure 4. Linear superposition predicts wing, but not head responses. (*a*) An unweighted sum of the ETA for the clockwise visual-stimulation-only response and the ETA for the haltere-stimulation-only response (Black triangle: magnet energizes. Grey triangle: magnet de-energizes) create a composite response (dark purple) that strongly predicts the experimentally observed multisensory ETA (red). A conventional linear model with weighted coefficients (light purple) that incorporates the same predictors shows only marginal improvement in predictive validity. (*b,c*) Same but for the contralateral wing and head clockwise responses respectively, with observed multisensory ETA shown in colours matching figures 2 and 3. (*d–f*) Same as (*a–c*) but for anticlockwise responses. (*g*) An unweighted model (dark purple) averaging both experimentally observed multisensory ETAs (clockwise and anticlockwise) strongly predicts the observed haltere-stimulation-only ipsilateral wing response. A conventional weighted linear model (light purple) shows only marginal improvement in predictive validity. (*h*) Same as (*g*) but for contralateral wing, showing low predictive validity for both models as this response is predominately uncorrelated with the stimulus. (*i*) Same as (*g*) and (*h*) but for head, showing inability to recover the unisensory response from the multisensory predictors for either class of model. (Online version in colour.)

While the haltere-only ETA was a significant predictor for both the clockwise (electronic supplementary material, table S1) and anticlockwise multisensory head response models (electronic supplementary material, table S2), neither the weighted nor unweighted average of multisensory predictors captured the unisensory haltere-evoked head response (figure 4*i*, electronic supplementary material, table S3). This may simply be because of the comparatively small average effect size of the haltere versus the visual input, which makes it unlikely for a model to recover this feature. More likely, this reflects a different motor output schema for the head versus the wing response. Recordings in blowflies show that some neck motoneurons cannot be driven to spike by haltere or visual inputs individually, but only by concurrent input from both [10]. Additionally, flies with ablated or immobilized halteres cannot modulate the gain of visually evoked head-steering responses [26], and recent work using systems identification methods suggests that head movement

responses to low-frequency visual stimuli are governed by a predictive control logic that is not shared with the wings [34].

As in haltere-stimulation-only trials, the magnetic stimulus was accompanied by a transient increase in instantaneous wingbeat frequency for both clockwise and anticlockwise trials. The response following this initial transient, however, showed considerable diversity between the stimulus conditions and was not well-described by a linear superposition of the individual visual and haltere responses (electronic supplementary material, figure S6). These findings are congruent with previous work showing that wingbeat amplitude and frequency components of both haltere- and visually evoked body rotations are modulated independently [22].

(d) Linear models predict the responses of individual flies as well as the mean

Our models perform well for predicting the mean responses of the six flies that exhibited qualitatively similar response profiles and completed all stimulus categories (i.e. all of their kinematic responses were in the same direction). However, this analysis does not capture the individual variation we observed, nor does it include two flies that showed a consistent opposite-direction response in one or more of the kinematic measures. Furthermore, fast responses particular to each animal may be lost in the group average. To address this, we produced models using ETAs computed from the replicate trials of individual flies, rather than the group. Electronic supplementary material, figure S7A–H shows the results of this modelling for the six flies included in figure 4, as well as for the two flies which exhibited atypical response profiles.

Several of these single-fly analyses (electronic supplementary material, figure S7A, B, and H for flies 1, 5 and 12, respectively) achieve consistently high levels of predictive validity across kinematic parameters and stimulus classes, in some cases comparable to the models derived from the population mean. Notably, this approach was also successful in predicting some of the responses of the two individuals with divergent behaviours. In addition to the typical decrease in ipsilateral wing amplitude, fly 8 (electronic supplementary material, figure S7E) responded to the magnetic stimulation with a reversed head-steering response and a large decrease in the contralateral wing amplitude. The linear summation model performed adequately for this fly's head and wing responses—but only for the clockwise visual stimulus. Neither the unweighted summation model nor the weighted multiple regression model predicts the head responses to the anticlockwise stimulus. Furthermore, this fly's head and wing responses were not symmetric with respect to the sign of the stimulus, as illustrated by averaging the two directional classes of multisensory ETA.

In other flies, the models were less predictive. In fly 9 (electronic supplementary material, figure S7F), this was directly attributable to an insufficient number of replicate trials for the unisensory haltere parameter estimate ($n = 3$). In other flies, this coincides with a smaller response magnitude for one of the two sense modalities. Fly 6, which was excluded from the main dataset because of its reversed ipsilateral wing response (electronic supplementary material, figure S7C), evidences very little response magnitude for either directional category of visual stimulus, and fly 11 (electronic supplementary material, figure S7G) shows only initial offset transients in the head and wing responses to the haltere stimulus. For the majority of kinematic parameters and stimulus classes, the models are unable to predict the responses of these flies because they are not different from noise.

These single-animal models support two key inferences. First, a linear superposition of haltere and visual responses sufficiently explains the responses of several individual animals using parameter estimates drawn from considerably fewer replicate trials than in the analysis of the wider dataset (no more than twelve for any parameter for any animal), suggesting that the model fit to the population average is not an artefact of averaging. Second, the model works well for certain stimulus classes in a fly with a qualitatively different response profile, implying that it reflects general rules for the fly's nervous system within a broad region of its operational range.

3. Discussion

We have introduced a method for reproducibly altering haltere stroke kinematics of flies in tethered flight and have used it to quantify the integration of visual and haltere sensory inputs for wing and gaze equilibrium reflexes, thereby following the complete transformation of stimulus information into behavioural outputs. In *Drosophila*, visual and haltere sensory inputs direct wing-steering manoeuvres through the coordinated activity of four anatomically distinct groups of muscles that alter mechanical properties of the wing hinge—one group of basalary muscles and three groups of axillary muscles [20,35]. Each group contains both wingbeat-synchronous and wingbeat-asynchronous muscles, for mediating large transient and small continuous changes in steering amplitude, respectively [35]. Halteres also possess a set of steering muscles which receive descending visual information [11,20], and thus haltere input to the wings includes this indirect input from the visual system. Using these muscles in concert with the large power muscles driving the wingstroke, the fly is capable of independently modulating wingbeat frequency and wingbeat amplitude. We directly demonstrate that imposed changes in haltere biomechanics are sufficient to reproduce the acute phase changes in the wing motor system observed in previous research [12,20].

While encoding properties of individual haltere campaniform sensilla are well-characterized [3,7,8], two major impediments currently limit a complete understanding of the contribution of haltere sensory information to the fly thoracic nervous system. First, campaniform sensilla at the haltere base are organized into anatomically distinct fields [5], the functions of which are still hypothetical. To date, only field dF2 has been linked with a synaptic target in the blowfly *Calliphora*—the motoneuron controlling the first basilar muscle [9]. Second, information about the downstream processing of haltere information is lacking. Though several contralateral haltere interneurons (cHINs) have been identified, linking haltere sensors to contralateral wing and neck motoneurons[13,19], these have not been characterized physiologically, nor has any anatomical pattern been observed as to which populations of haltere campaniform sensilla comprise their synaptic inputs. An experimental strategy combining our direct manipulation of haltere kinematics with the array of *Drosophila* genetic tools for manipulations of neural circuits may help characterize this sensorimotor pathway. Indeed, a similar approach has recently identified and characterized functional populations of leg proprioceptors and their accompanying thoracic interneurons [36].

Though the complete encoding scheme through which haltere movement information is represented in the nervous system remains unresolved, our findings outline the sensorimotor transformations mediated by the haltere system and quantify the effects of haltere input on behaviour. We show that visually evoked and haltere-evoked changes in wing-stroke amplitude sum linearly as a superposition of states, while gaze responses do not. A similar disparity between wing-steering and gaze control has been observed in behavioural responses to differential figure/ground visual motion, with the wing response also following a linear integration logic and the gaze response ignoring figure motion entirely in the presence of ground motion [37]. These and other findings (including the present work) illustrate how the combined activity of nervous system elements with intrinsically nonlinear operating characteristics nevertheless mediate a linear sensorimotor transformation over the behaviourally relevant operating range [37,38].

4. Methods

(a) Flies and treatments

Adult female *Drosophila melanogaster*, aged 3–5 days post-eclosion, were reared from a colony of wild-caught flies. Flies were cold-anaesthetized and tethered to tungsten pins for flight experiments. For magnetic stimulation experiments, a single iron filing was attached to one of the two halteres with UV-curing dental cement. For some flies in the bulb loading experiments show in figure 1*b*, the UV-curing cement was used by itself to add mass to the haltere bulb. All animals were treated on the right haltere.

For weighting experiments using iron filings, masses were estimated by tracing the cross-sectional area of the filing from a single video frame and calculating the mass of an iron sphere with an equivalent cross-sectional area. For weighting experiments with glued halteres, equivalent spherical volumes were calculated from the sectional area of the glue mass, as well as the contralateral untreated haltere bulb. By subtracting the latter volume from the former, an estimate of the glue volume was obtained. The estimated mass of this resultant volume was calculated using the manufacturer's published value for the glue's specific gravity (accessed at: https://www.henkel-adhesives.com/us/en/product/uv-adhesives-_-light-cure-adhesives/loctite_aa_3972.html)

(b) Magnetic stimulation

To facilitate control over haltere stroke parameters, an iron-core electromagnet was positioned posterior and ventral to the flying, tethered *Drosophila* (figure 1*a*) The electromagnet was powered from a variable power supply (TP1803D, Tekpower, Montclair, CA, USA) switched through a transistor (D1276A, Panasonic, Kadoma, Japan) and controlled via 5 V TTL-level output from a data acquisition board (USB-6434, National Instruments, Austin TX, USA). The field intensity at the fly's body was approximately 2000 µT, which exceeded the measurement range of our instrument (HMC5883 L Magnetometer, Honeywell, Plymouth MN, USA) and so was calculated from a measurement series at distance (electronic supplementary material, figure S1). For the control experiments investigating the effects of magnetic fields on untreated flies, a second nearly identical magnet was placed dorsal and anterior to the fly, controlled with its own power supply, and switched through its own power transistor to provide a field of similar magnitude but opposite in sign.

Subsequent to tethering, we monitored each experimental fly in real time through our high-speed camera set-up to ensure that the treated haltere maintained a naturalistic amplitude and phase synchrony with the wing. The precise positioning of the electromagnet relative to the tethered fly, as well as the current and voltage settings for the power supply, was then adjusted empirically for each fly to ensure that a test pulse of the magnetic stimulation produced the maximum effect on each filing-treated haltere. The recording did not proceed unless these criteria were met. Activation of the magnetic stimulation occasionally resulted in the cessation of tethered flight or provoked a haltere grooming response with the metathoracic leg, and these trials were not included in the dataset.

(c) Visual stimulation

Concurrent with magnetic stimulation, one of several visual stimuli was presented to the fly using an LED flight arena. To assess baseline behavioural and kinematic responses to magnetic stimulation, the fly was recorded with the LED panels in the flight arena turned off or with uniform activation of all the LED panels in the arena. To elicit yaw optomotor head and wing responses and assess multisensory integration of vision and haltere sensory information, we presented flies with wide-field grating patterns comprised of random stripes each with a width no more than 15°. This grating pattern moved left and right with a 1 Hz triangle-wave motion at a pattern velocity of 90°/s, parameters which were identified in [26] as eliciting a robust optomotor response from both the head and the wings. The phase of the visual stimulus triangle-wave was adjusted such that the magnetic stimulation epochs occurred either during clockwise pattern motion (towards the treated haltere) or anticlockwise pattern motion (away from the treated haltere). Magnet pulses were activated at a rate of 2 Hz to provide interleaved magnet-off control visual trials.

(d) High-speed video and machine vision

Two high-speed cameras (TS4 or IL5, Fastec Imagining, San Diego, CA, USA) were trained on the lateral aspects of the fly and captured video at 1000 or 2000 Hz. An additional high-speed industrial camera (Point Grey Chameleon3, FLIR, Wilsonville, OR, USA) viewed the fly from above, sampling at a rate of 100 Hz. Shutters for the two lateral cameras were synchronized and shutter signals from all three cameras were sampled at 10 000 Hz on the DAQ to facilitate alignment of the recorded videos with one another and with control signals for the visual and magnetic stimulation.

A standalone MATLAB program (https://github.com/michaelrauscher/flyalyzer) was developed for offline tracking of head orientation in the yaw plane and estimation of the left and right wing downstroke envelopes from the overhead-view camera. Haltere and wing angular position was extracted from the lateral aspect videos using the DeepLabCut pose-estimation software package [39].

(e) High-speed video analysis

Instantaneous stroke frequencies were derived from band-pass filtered (100–600 Hz window) joint angle time series using the Hilbert transform, and smoothed using a 100 sample moving average filter. Wing and haltere stoke amplitude and wing–haltere phase delay for each trial epoch (figure 1*f–g*) were measured in the time domain using a peak detection algorithm on the filtered time series.

(f) Modelling

Custom MATLAB scripts were used to produce ETAs, model fits and ANOVA statistics. For both unweighted and weighted models, predictor variables consisted of 100 sample ETAs from

the focal kinematic parameter and stimulus classes. Models took the form of a standard linear regression model:

$$\hat{y} = \beta_0 + \beta_1 x_1 + \beta_2 x_2$$

$\hat{y}$ is the predicted value of the model, β_0 is a fixed intercept term and β_1 and β_2 are scaling coefficients of the two predictors, x_1 and x_2. For the unweighted summation models, only the intercept β_0 was fit to the data to minimize least-squares error. For unweighted models predicting the multisensory response from the individual unisensory responses, β_1 and β_2 were each locked at 1 to reflect the simple arithmetic sum of the two predictor ETAs. For unweighted models predicting the unisensory haltere-evoked response from the two-directional classes of multisensory responses, β_1 and β_2 were each locked at 0.5 to reflect the simple arithmetic mean of the two predictor ETAs. For the weighted linear models, a standard least-squares fitting process was used with all β coefficients unlocked. The propagated error was computed for both weighted and unweighted models by summing the standard error for each ETA in quadrature, and confidence intervals computed from these with effective degrees of freedom determined using the Welch–Satterthwaite method.

Data accessibility. Data are available from the Dryad Digital Repository: https://doi.org/10.5061/dryad.g4f4qrfnr [40].

Authors' contributions. M.J.R. designed the study, collected data, analysed data and drafted the manuscript. J.L.F. obtained funding, designed the study, coordinated the study and revised the manuscript.

Competing interests. We declare we have no competing interests.

Funding. This work was supported by United States Air Force Office of Scientific Research Grants FA9550-14-0398 and FA9550-16-1-0165 and National Science Foundation award 1754412 to J.L.F.

Acknowledgements. We would like to thank Chenxin Bi for help with data collection, Noah DeFino and Jesse Fritz for animal care and Alexandra Yarger, Nicholas Kathman, Jeremy Didion, Hillel Chiel, Roy Ritzmann, David Bertsch and Gabriella Wolff for helpful commentary.

References

1. Rauscher MJ, Fox JL. 2018 Inertial sensing and encoding of self-motion: structural and functional similarities across metazoan taxa. *Integr. Comp. Biol.* **58**, 832–843. (doi:10.1093/icb/icy041)
2. Derham W. 1714 *Physico-theology: or, a demonstration of the being and attributes of God, from His works of creation. Being the substance of XVI sermons preached in St. Mary Le Bow-church, London, at the honble Mr. Boyle's lectures, in the years 1711 and 1712*. W. and J. Innys, London, 1714. See https://archive.org/details/physicotheologyo00derh
3. Pringle JWS. 1948 The gyroscopic mechanism of the halteres of Diptera. *Phil. Trans. R. Soc. B* **233**, 347–384. (doi:10.1098/rstb.1948.0007)
4. Agrawal S, Grimaldi D, Fox JL. 2017 Haltere morphology and campaniform sensilla arrangement across Diptera. *Arthropod Struct. Dev.* **46**, 215–229. (doi:10.1016/j.asd.2017.01.005)
5. Gnatzy W, Grünert U, Bender M. 1987 Campaniform sensilla of *Calliphora vicina* (Insecta, Diptera). *Zoomorphology* **106**, 312–319. (doi:10.1007/BF00312005)
6. Smith DS. 1969 The fine structure of haltere sensilla in the blowfly, *Calliphora erythrocephala* (meig.), with scanning electron microscopic observations on the haltere. *Tissue Cell* **1**, 443–484. (doi:10.1016/S0040-8166(69)80016-9)
7. Yarger AM, Fox JL. 2018 Single mechanosensory neurons encode lateral displacements using precise spike timing and thresholds. *Proc. R. Soc. B* **285**, 20181759. (doi:10.1098/rspb.2018.1759)
8. Fox JL, Daniel TL. 2008 A neural basis for gyroscopic force measurement in the halteres of *Holorusia*. *J. Comp. Physiol. A Neuroethol. Sensory, Neural, Behav. Physiol.* **194**, 887–897. (doi:10.1007/s00359-008-0361-z)
9. Fayyazuddin A, Dickinson MH. 1996 Haltere afferents provide direct, electrotonic input to a steering motor neuron in the blowfly, *Calliphora*. *J. Neurosci.* **16**, 5225–5232. (doi:10.1523/JNEUROSCI.16-16-05225.1996)
10. Huston SJ, Krapp HG. 2009 Nonlinear integration of visual and haltere inputs in fly neck motor neurons. *J. Neurosci.* **29**, 13 097–13 105. (doi:10.1523/JNEUROSCI.2915-09.2009)
11. Chan WP, Prete F, Dickinson MH. 1998 Visual input to the efferent control system of a fly's 'gyroscope'. *Science* **280**, 289–292. (doi:10.1126/science.280.5361.289)
12. Fayyazuddin A, Dickinson MH. 1999 Convergent mechanosensory input structures the firing phase of a steering motor neuron in the blowfly, *Calliphora*. *J. Neurophysiol.* **82**, 1916–1926. (doi:10.1152/jn.1999.82.4.1916)
13. Strausfeld NJ, Seyan HS. 1985 Convergence of visual, haltere, and prosternal inputs at neck motor neurons of *Calliphora erythrocephala*. *Cell Tissue Res.* **240**, 601–615. (doi:10.1007/BF00216350)
14. Suver MP, Huda A, Iwasaki N, Safarik S, Dickinson MH. 2016 An array of descending visual interneurons encoding self-motion in *Drosophila*. *J. Neurosci.* **36**, 11 768–11 780. (doi:10.1523/JNEUROSCI.2277-16.2016)
15. Namiki S, Dickinson MH, Wong AM, Korff W, Card GM. 2018 The functional organization of descending sensory-motor pathways in *Drosophila*. *Elife* **7**, e34272. (doi:10.7554/eLife.34272)
16. Bartussek J, Lehmann F-O. 2016 Proprioceptive feedback determines visuomotor gain in *Drosophila*. *R. Soc. Open Sci.* **3**, 150562. (doi:10.1098/rsos.150562)
17. Bartussek J, Lehmann F-O. 2018 Sensory processing by motoneurons: a numerical model for low-level flight control in flies. *J. R. Soc. Interface* **15**, 20180408. (doi:10.1098/rsif.2018.0408)
18. Milde JJ, Seyan HS, Strausfeld NJ. 1987 The neck motor system of the fly *Calliphora erythrocephala*. II. Sensory organization. *J. Comp. Physiol. A* **160**, 225–238. (doi:10.1007/BF00609728)
19. Trimarchi JR, Murphey RK. 1997 The shaking-B2 mutation disrupts electrical synapses in a flight circuit in adult *Drosophila*. *J. Neurosci.* **17**, 4700–4710. (doi:10.1523/JNEUROSCI.17-12-04700.1997)
20. Dickerson BH, de Souza AM, Huda A, Dickinson MH. 2019 Flies regulate wing motion via active control of a dual-function gyroscope. *Curr. Biol.* **29**, 3517–3524. (doi:10.1016/j.cub.2019.08.065)
21. Dickinson MH. 1999 Haltere-mediated equilibrium reflexes of the fruitfly, *Drosophila melanogaster*. *Phil. Trans. R. Soc. B* **354**, 903–916. (doi:10.1098/rstb.1999.0442)
22. Sherman A, Dickinson MH. 2003 A comparison of visual and haltere-mediated equilibrium reflexes in the fruit fly *Drosophila melanogaster*. *J. Exp. Biol.* **206**, 295–302. (doi:10.1242/jeb.00075)
23. Sherman A, Dickinson MH. 2004 Summation of visual and mechanosensory feedback in *Drosophila* flight control. *J. Exp. Biol.* **207**, 133–142. (doi:10.1242/jeb.00731)
24. Mureli S, Fox JL. 2015 Haltere mechanosensory influence on tethered flight behavior in *Drosophila*. *J. Exp. Biol.* **210**, 2528–2537. (doi:10.1242/jeb.121863)
25. Hengstenberg R. 1988 Mechanosensory control of compensatory head roll during flight in the blowfly *Calliphora erythrocephala* Meig. *J. Comp. Physiol. A* **163**, 151–165. (doi:10.1007/BF00612425)
26. Mureli S, Thanigaivelan I, Schaffer ML, Fox JL. 2017 Cross-modal influence of mechanosensory input on gaze responses to visual motion in *Drosophila*. *J. Exp. Biol.* **220**, 2218–2227. (doi:10.1242/jeb.146282)
27. Bender JA, Dickinson MH. 2006 A comparison of visual and haltere-mediated feedback in the control of body saccades in *Drosophila melanogaster*. *J. Exp. Biol.* **209**, 4597–4606. (doi:10.1242/jeb.02583)
28. Nalbach G. 1993 The halteres of the blowfly *Calliphora*. *J. Comp. Physiol. A* **173**, 293–300. (doi:10.1007/BF00212693)

29. Thompson RA, Wehling MF, Evers JH, Dixon WE. 2009 Body rate decoupling using haltere mid-stroke measurements for inertial flight stabilization in Diptera. *J. Comp. Physiol. A Neuroethol. Sensory, Neural, Behav. Physiol.* **195**, 99–112. (doi:10.1007/s00359-008-0388-1)
30. Hall JM, McLoughlin DP, Kathman ND, Yarger AM, Mureli S, Fox JL. 2015 Kinematic diversity suggests expanded roles for fly halteres. *Biol. Lett.* **11**, 20150845. (doi:10.1098/rsbl.2015.0845)
31. Deora T, Singh AK, Sane SP. 2015 Biomechanical basis of wing and haltere coordination in flies. *Proc. Natl Acad. Sci. USA* **112**, 1481–1486. (doi:10.1073/pnas.1412279112)
32. Deora T, Sane SP. 2020 The coupled dual-oscillator model of wing and haltere motion in flies. *bioRxiv*, 2020.03.08.982520. (doi:10.1101/2020.03.08.982520)
33. Kim AJ, Fenk LM, Lyu C, Maimon G, Otsuna H, Ito K, Borst A, Reiff DF. 2017 Quantitative predictions orchestrate visual signaling in *Drosophila*. *Curr. Biol.* **168**, 280–294. (doi:10.1016/j.cell.2016.12.005)
34. Cellini B, Mongeau JM. 2020 Active vision shapes and coordinates flight motor responses in flies. *Proc. Natl Acad. Sci. USA* **117**, 23 085–23 095. (doi:10.1073/pnas.1920846117)
35. Lindsay T, Sustar A, Dickinson M. 2017 The function and organization of the motor system controlling flight maneuvers in flies. *Curr. Biol.* **27**, 345–358. (doi:10.1016/j.cub.2016.12.018)
36. Agrawal S, Dickinson E, Sustar A, Gurung P, Shepherd D, Truman J, Tuthill J. 2020 Central processing of leg proprioception in *Drosophila*. *Elife* **9**, e60299.
37. Fox JL, Frye MA. 2014 Figure-ground discrimination behavior in *Drosophila* II. Visual influences on head movement behavior. *J. Exp. Biol.* **217**, 570–579. (doi:10.1242/jeb.080192)
38. Theobald JC, Ringach DL, Frye MA. 2010 Dynamics of optomotor responses in *Drosophila* to perturbations in optic flow. *J. Exp. Biol.* **213**, 1366–1375. (doi:10.1242/jeb.037945)
39. Mathis A, Mamidanna P, Cury KM, Abe T, Murthy VN, Mathis MW, Bethge M. 2018 DeepLabCut: markerless pose estimation of user-defined body parts with deep learning. *Nat. Neurosci.* **21**, 1281–1289. (doi:10.1038/s41593-018-0209-y)
40. Rauscher MJ, Fox JL. 2018 Weighted haltere and imposed haltere stroke reduction tethered flying *Drosophila* kinematics. Dryad Digital Repository. (doi:10.5061/dryad.g4f4qrfnr)